Electronic supplementary information

High-performance ternary organic solar cells with photoresponses beyond 1000 nm

Peiyao Xue,[a] Yiqun Xiao,[b] Tengfei Li,[a] Shuixing Dai,[a] Boyu Jia,[a] Kuan Liu,[a] Jiayu Wang,[a] Xinhui Lu,[b] Ray P.S. Han,[a,*] and Xiaowei Zhan[a,*]

[a]Department of Materials Science and Engineering, College of Engineering, Key Laboratory of Polymer Chemistry and Physics of Ministry of Education, Peking University, Beijing, 100871, P. R. China.

[b]Department of Physics, The Chinese University of Hong Kong, New Territories 999077, Hong Kong, P. R. China

Materials

F8IC[S1] and IDT-2BR[S2] were synthesized according to reported procedures. PTB7-Th (M_w = 124 kDa, M_w/M_n = 1.7) was purchased from 1-Materials Inc.; chloroform (99.9%), diphenyl ether (DPE) (99.5%) and 2-methoxyethanol (99.8%) were purchased from J&K Chemical Inc.; zinc acetate dihydrate (99.9%), ethanolamine (99.5%) and MoO_3 were purchased from Sigma-Aldrich Inc.; and all the solvents and chemicals were used without further purification.

Characterization

The ultraviolet-visible (UV-vis) absorption spectra were measured on JASCO V-570 spectrophotometer in thin film (on a quartz substrate). Emission spectra were recorded on Hitachi F-4500 spectrophotometer (for samples with emission wavelength < 900 nm) or FLS980 fluorescence spectrophotometer (Edinburgh Instrument Co., Ltd., for samples with emission wavelength > 900 nm). Electrochemical measurements were carried out under argon in a deoxygenated solution of tetra-butylammonium hexafluorophosphate (0.1 M) in acetonitrile using a potential scan rate of 100 mV s^{-1} with a computer-controlled CHI660C electrochemical workstation, a glassy-carbon working electrode coated with films, a platinum-wire auxiliary electrode and a Ag/AgCl electrode as a reference electrode. The potentials were referenced to a ferrocenium/ferrocene ($FeCp_2^{+/0}$) couple using ferrocene as an external standard. The HOMO and LUMO energies are estimated from the onset oxidation (E_{ox}) and reduction potentials (E_{red}) versus $FeCp_2^{+/0}$ (0.45 V vs. Ag/AgCl), respectively, assuming the absolute energy level of $FeCp_2^{+/0}$ to be 4.8 eV below vacuum.

$$\text{HOMO} = -e\,(E_{ox} - 0.45) - 4.8\ (\text{eV})$$

$$\text{LUMO} = -e\,(E_{red} - 0.45) - 4.8\ (\text{eV})$$

The morphology was observed using a Multimode 8 scanning probe microscopy (Bruker Daltonics) in the tapping mode and a JEM-2100 transmission electron microscope (TEM) operated at 200 keV. The grazing incidence wide-angle X-ray scattering (GIWAXS) and the grazing incidence small-angle X-ray scattering (GISAXS) measurements were carried out at BL23A1 of National Synchrotron Radiation Research Center, Hsinchu. The energy of the X-ray source was set to 10 keV (wavelength of 1.24 Å) and the incident angle was 0.15°. Both GIWAXS and GISAXS samples are prepared on silicon substrate by spin coating.

Device fabrication and characterization

All the devices are based on inverted sandwich structure, ITO glass/ZnO/active layer/MoO_x/Ag. First, the patterned indium tin oxide (ITO) glass (sheet resistance = 15 Ω □$^{-1}$) was precleaned in the ultrasonic bath with de-ionized water, acetone and isopropanol. Then, a ZnO layer (*ca.* 30 nm) was spin-coated at 4000 rpm onto the ITO glass from ZnO precursor solution (prepared by dissolving 0.1 g of zinc acetate dihydrate ($Zn(CH_3COO)_2{\cdot}2H_2O$) and 0.03 mL of ethanolamine ($NH_2CH_2CH_2OH$) in 1.0 mL of 2-methoxyethanol ($CH_3OCH_2CH_2OH$)), followed by baking at 200 °C for 30 min. After that, the photoactive layer consisting of PTB7-Th/acceptors mixture solution (10.0 mg mL^{-1}) in chloroform was spin-coated at 1400 rpm onto the ZnO layer (*ca*. 100 nm, measured by profilometer (Dektak XT)). A MoO_3 layer (*ca*. 5 nm) and Ag layer (*ca.* 80 nm) were then evaporated onto the active layer under the vacuum (*ca.* 10^{-5} Pa) to form the anode electrode. The measured area of the active device was 4 mm^2. The current density-voltage (*J-V*) curve was measured using a computer-controlled B2912A Precision Source/Measure Unit (Agilent Technologies). An XES-70S1 (SAN-EI Electric Co., Ltd) solar simulator (AAA grade, 70 × 70 mm^2 photobeam

size) coupled with AM 1.5G solar spectrum filters was used as the light source, and the optical power at the sample was 100 mW cm^{-2}. A 2 × 2 cm^2 monocrystalline silicon reference cell (SRC-1000-TC-QZ) was purchased from VLSI Standards Inc. The external quantum efficiency (EQE) spectrum was measured using a Solar Cell Spectral Response Measurement System QE-R3011 (Enlitech Co., Ltd.). The light intensity at each wavelength was calibrated using a standard single crystal Si photovoltaic cell.

SCLC measurement

Hole-only and electron-only devices were fabricated using the architectures ITO glass/PEDOT:PSS/active layer/Au for holes and ITO glass/ZnO/active layer/Ca/Al for electrons. For hole-only devices, the pre-cleaned ITO glass was treated by ultraviolet-ozone chamber (UVO) (Jelight Company, USA) for 15 min. Then PEDOT:PSS (*ca*. 35 nm) was spin-coated on it, and baked at 150 °C in the drying oven for 15 min. The photoactive layer was spin-coated at 1400 rpm on PEDOT:PSS layer, and Au (*ca*. 80 nm) was evaporated onto the photoactive layer under vacuum. For electron-only devices, ZnO (*ca*. 30 nm) was spin-coated onto the ITO glass, then the photoactive layer was spin-coated at 1400 rpm on ZnO. At the end, Ca (*ca*. 10 nm) and Al (*ca*. 80 nm) were evaporated under vacuum. The mobility was extracted by fitting the current density-voltage curves using space charge limited current (SCLC). The equation is as follows

$$J = (9/8)\mu\varepsilon_r\varepsilon_0 V^2 \exp(0.89(V/E_0L)^{0.5})/L^3$$

where J refers to the current density, μ is hole or electron mobility, ε_r is relative dielectric constant, ε_0 is dielectric constant of free space, $V = V_{appl} - V_{bi}$, E_0 is characteristic field, L is the thickness of the active layer. L was measured by Dektak XT (Bruker).

Table S1 Performance of the OSCs with different IDT-2BR content in acceptors[a]

IDT-2BR (%)	DIO (% v/v)	V_{OC} (V)	J_{SC} (mA cm^{-2})	FF (%)	PCE (%)	calc J_{SC} (mA cm^{-2})
0	0.5	0.646 (0.645±0.006)	24.6 (24.5±0.4)	64.9 (63.5±1.8)	10.3 (10.1±0.3)	24.2
10	0.5	0.662 (0.660±0.003)	25.5 (25.5±0.5)	68.7 (67.3±1.4)	11.6 (11.3±0.3)	24.2
20	0	0.702 (0.702±0.003)	23.1 (22.2±0.8)	66.6 (66.6±1.3)	10.8 (10.4±0.4)	22.5
20	0.5	0.687 (0.683±0.006)	25.1 (25.3±0.7)	69.9 (68.6±1.1)	12.1 (11.9±0.3)	24.2
20	1	0.682 (0.680±0.011)	24.4 (22.8±1.8)	71.4 (70.7±2.8)	11.8 (10.9±0.8)	23.2
30	0.5	0.700 (0.701±0.003)	23.6 (23.5±0.5)	66.1 (64.4±2.0)	11.0 (10.6±0.4)	22.9
50	0.5	0.730 (0.731±0.002)	20.8 (20.8±0.3)	49.7 (47.3±2.3)	7.58 (7.20±0.41)	20.8
100	0.5	1.05 (1.05±0.006)	12.9 (13.0±0.4)	54.3 (53.0±1.9)	7.31 (7.21±0.09)	13.2

[a]Average values (in parenthesis) obtained from 15 devices.

Table S2 Hole mobilities and electron mobilities of blend films.

active layer	μ_h (cm^2 V^{-1} s^{-1})	μ_e (cm^2 V^{-1} s^{-1})	μ_h/μ_e
PTB7-Th/F8IC	4.5×10^{-4}	8.4×10^{-5}	5.4
PTB7-Th/IDT-2BR	1.3×10^{-5}	1.0×10^{-5}	1.3
PTB7-Th/F8IC/IDT-2BR	1.1×10^{-3}	6.4×10^{-4}	1.7

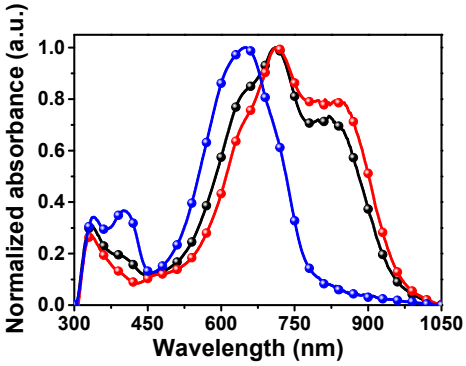

Fig. S1 Absorption spectra of PTB7-Th/IDT-2BR (blue), PTB7-Th/F8IC (red) and PTB7-Th/F8IC/IDT-2BR films (black).

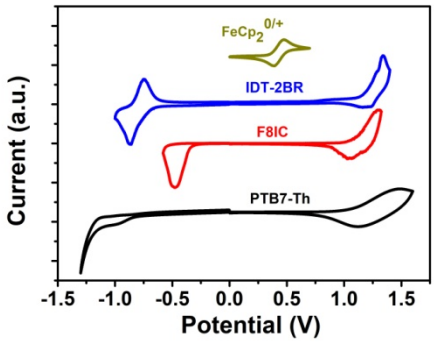

Fig. S2 Cyclic voltammograms of IDT-2BR, F8IC and PTB7-Th films in CH_3CN/0.1 M $[^nBu_4N]^+[PF_6]^-$ at 100 mV s^{-1}, the horizontal scale refers to an Ag/AgCl electrode.

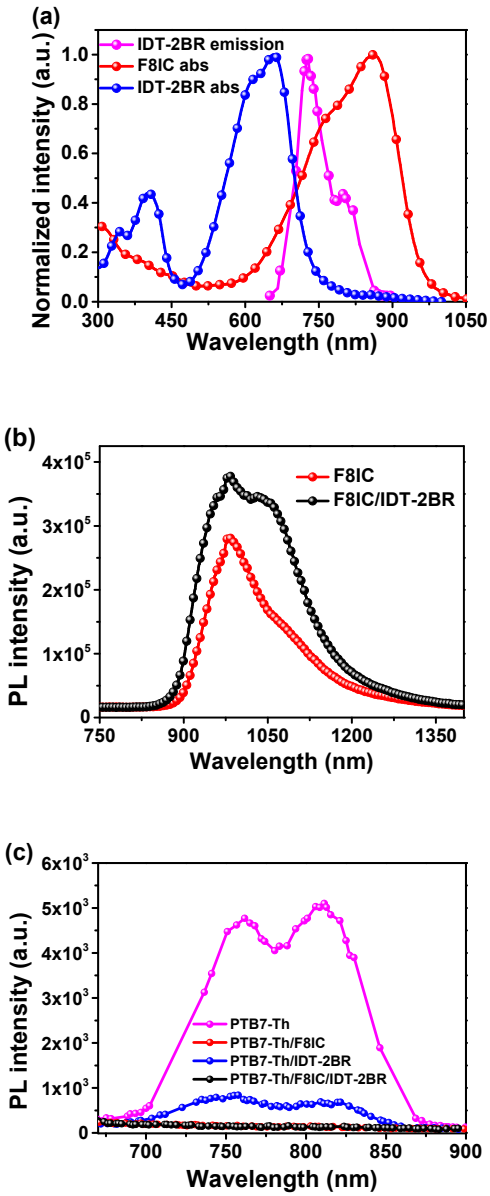

Fig. S3 (a) Normalized photoluminescence spectrum of IDT-2BR thin film and UV-vis absorption spectra of F8IC and IDT-2BR thin films. (b) Photoluminescence spectra of pure F8IC film and F8IC/IDT-2BR blend film. (c) Photoluminescence spectra of PTB7-Th, PTB7-Th/F8IC, PTB7-Th/IDT-2BR and PTB7-Th/F8IC/IDT-2BR films.

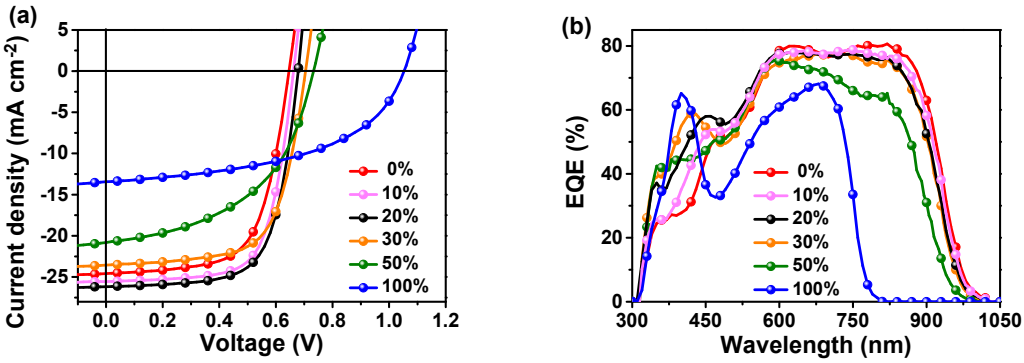

Fig. S4 (a) *J*–*V* characteristics and (b) EQE spectra of the OSCs with different IDT-2BR content.

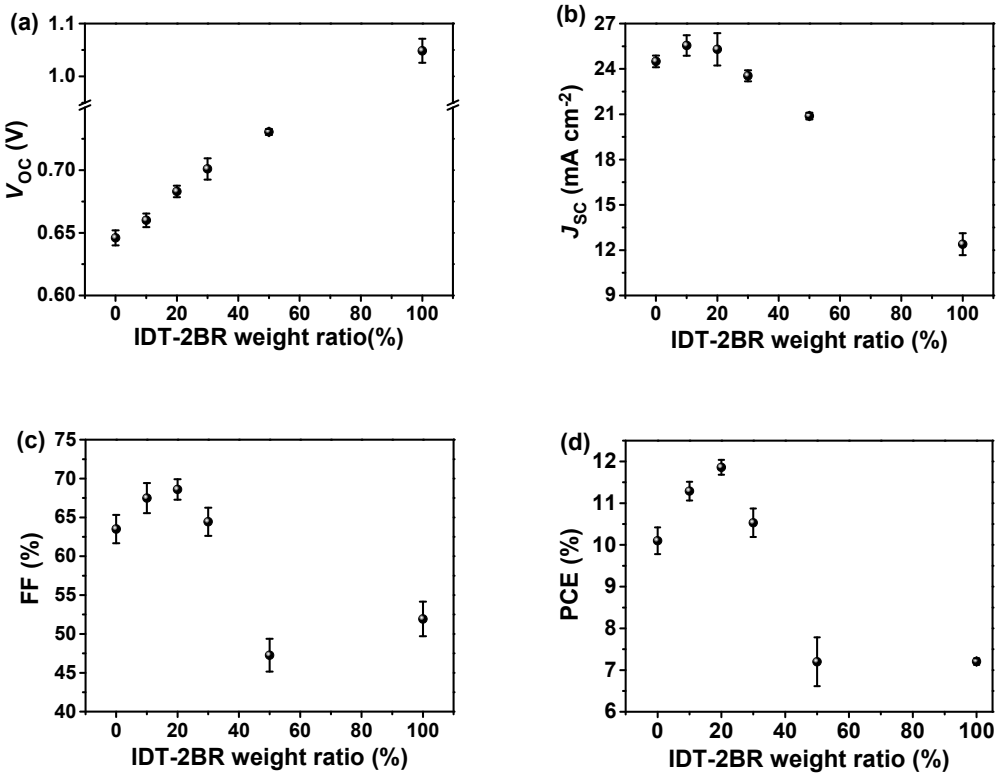

Fig. S5 (a) V_{OC}, (b) J_{SC}, (c) FF, and (d) PCE as a function of IDT-2BR weight ratio in acceptors.

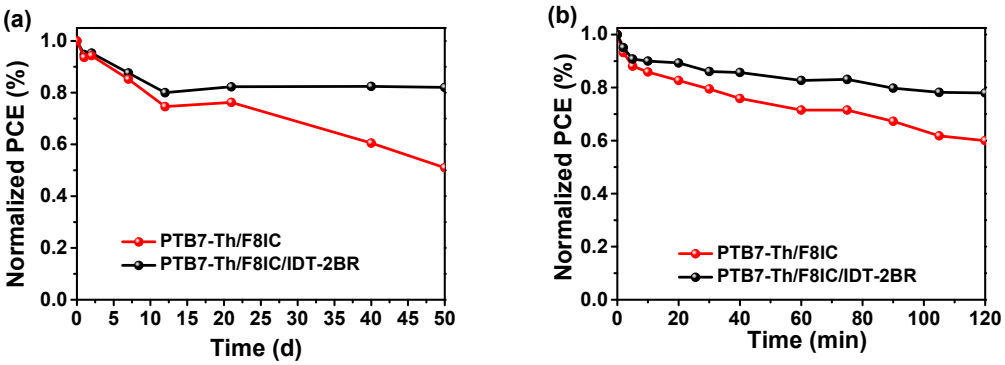

Fig. S6 Stability curves of PTB7-Th/F8IC and PTB7-Th/F8IC/IDT-2BR devices under air conditions (a) and continuous heating at 80 °C in nitrogen atmosphere (b).

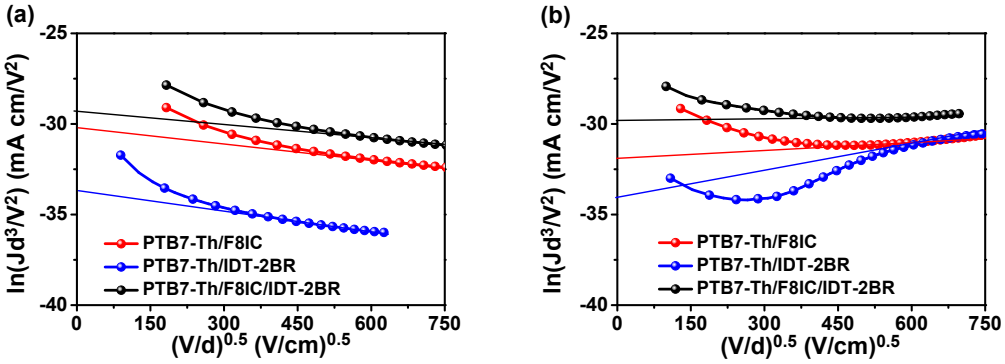

Fig. S7 *J-V* characteristics in the dark for hole-only (a) and electron-only (b) devices measured by SCLC method based on PTB7-Th/F8IC, PTB7-Th/IDT-2BR and PTB7-Th/F8IC/IDT-2BR blends.

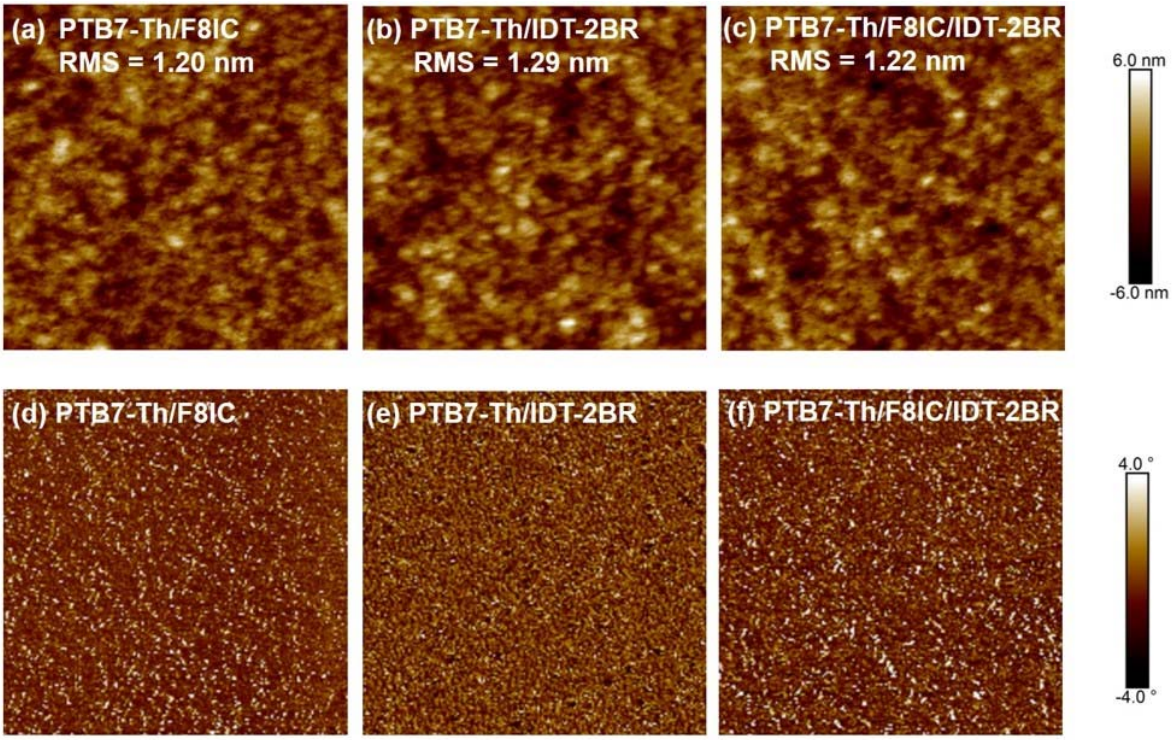

Fig. S8 AFM height images (2 μm × 2 μm) of (a) PTB7-Th/F8IC; (b) PTB7-Th/IDT-2BR; (c) PTB7-Th/F8IC/IDT-2BR blend films; phase images (2 μm × 2 μm) of (d) PTB7-Th/F8IC; (e) PTB7-Th/IDT-2BR; (f) PTB7-Th/F8IC/IDT-2BR blend films.

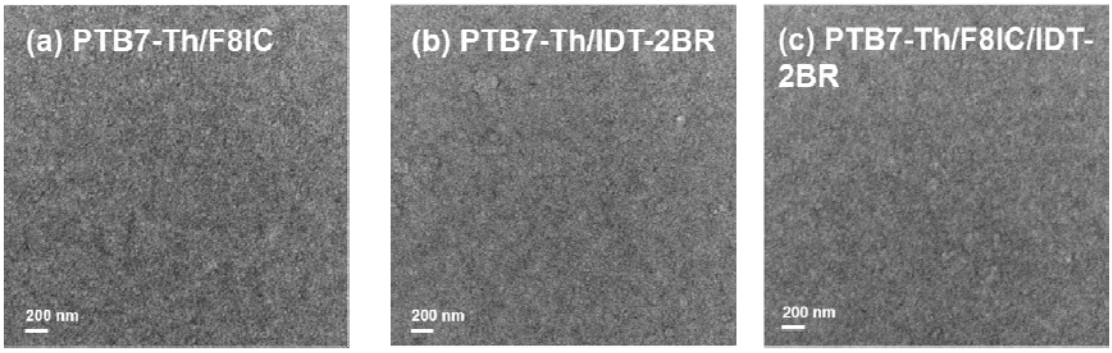

Fig. S9 TEM images of (a) PTB7-Th/F8IC; (b) PTB7-Th/IDT-2BR; (c) PTB7-Th/F8IC/IDT-2BR blend films.

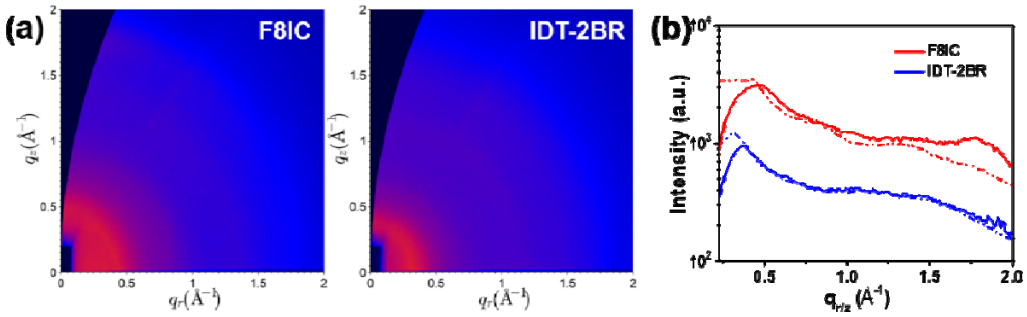

Fig. S10 (a) 2D GIWAXS patterns of the pure acceptors and (b) the corresponding intensity profile along the out-of-plane (solid lines) and in-plane (dashed lines) directions.

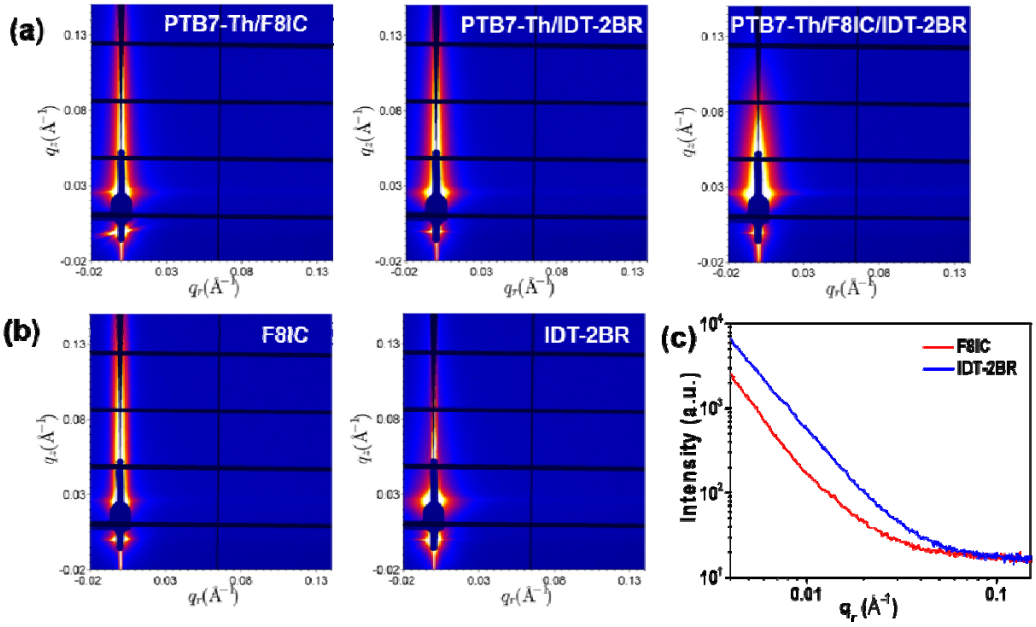

Fig. S11 (a) 2D GISAXS patterns of the blends. (b) 2D GISAXS patterns of the pure acceptors and (c) the corresponding intensity profile along the in-plane directions.

References

S1. S. Dai, T. Li, W. Wang, Y. Xiao, T.-K. Lau, Z. Li, K. Liu, X. Lu and X. Zhan, *Adv. Mater.*, 2018, **30**, 1706571.

S2. Y. Wu, H. Bai, Z. Wang, P. Cheng, S. Zhu, Y. Wang, W. Ma and X. Zhan, *Energy Environ. Sci.*, 2015, **8**, 3215-3221.